IOP Publishing Journal of Physics D: Applied Physics
J. Phys. D: Appl. Phys. **40** (2007) 4376–4381 doi:10.1088/0022-3727/40/14/037

Pulsed cooling of inhomogeneous thermoelectric materials

Q Zhou, Z Bian and A Shakouri[1]

Department of Electrical Engineering, University of California, Santa Cruz, CA 95064, USA

E-mail: ali@soe.ucsc.edu

Received 3 April 2007, in final form 23 May 2007
Published 29 June 2007
Online at stacks.iop.org/JPhysD/40/4376

Abstract
It has been proven that the maximum cooling temperature of a thermoelectric material can be increased by using either pulsed operation or graded Seebeck profiles. In this paper, we show that the maximum cooling temperature can be further increased by the pulsed operation of optimal inhomogeneous thermoelectric materials. A random sampling method is used to obtain the optimal electrical conductivity profile of inhomogeneous materials, which can achieve a much higher cooling temperature than the best uniform materials under the steady-state condition. Numerical simulations of pulsed operation are then carried out in the time domain. In the limit of low thermoelectric figure-of-merit *ZT*, the finite-difference time-domain simulations are verified by an analytical solution for homogeneous material. This numerical method is applied to high *ZT* BiTe materials and simulations show that the effective figure-of-merit can be improved by 153% when both optimal graded electrical conductivity profiles and pulsed operation are used.

1. Introduction

Thermoelectric coolers can pump heat using electricity without any moving parts. They are lightweight, small and inexpensive. The steady-state cooling temperature of a homogeneous thermoelectric material is limited by its dimensionless thermoelectric figure-of-merit $ZT = S^2\sigma T/K$, where S is the Seebeck coefficient; T is the absolute temperature and σ and K are the electrical and thermal conductivities, respectively. It is a challenge to find a material with a large *ZT* which can offer deep cooling down to cryogenic temperatures.

It is well known that maximum cooling temperature can be increased by using pulsed operation of a thermoelectric cooler. Peltier cooling occurs at the cold junction while Joule heating is distributed in the body of the thermoelectric element. The Joule heating takes more time than the Peltier cooling to affect the temperature at the cold side due to the finite heat diffusion time. Thus, one can produce a transient cold spike by superimposing an additional current pulse on the original optimal current for steady-state operation. The first studies of thermoelectric cooling in a non-stationary mode were reported in [1, 2]. Recently, the transient behaviour of thermoelectric coolers has been studied in detail theoretically and experimentally [3]. Various shapes of the thermoelectric devices and different forms of the current pulse are also investigated to get the highest pulsed cooling and longest cooling duration [4–6]. Transient cooling can be used in applications that need extra cooling—larger than the maximum steady-state value—for a short time. Typical applications are infrared detectors, condensation hygrometers and the super-cooling of nozzles and tubes in a conventional refrigerator, etc [4]. It is also possible to achieve continuous cooling with pulsed enhancement by using a MEMS device [7]. In this interesting design, the cooled target is in thermal contact with the pulsed cooling device only during the lowest temperature cycles.

Recently graded thermoelectric materials were proposed to provide much larger cooling temperatures and efficiencies due to distributed Peltier cooling [8, 9]. The maximum steady-state cooling temperature of practical thermoelectric materials such as BiTe is typically increased by 20–30% when the optimal graded material profile is used [10, 11]. In this paper, we present a numerical study of pulsed cooling for an optimally graded thermoelectric material and show that a cooling temperature larger than any of the three cases studied before is possible, i.e. larger than (1) steady-state cooling of

[1] Author to whom any correspondence should be addressed.

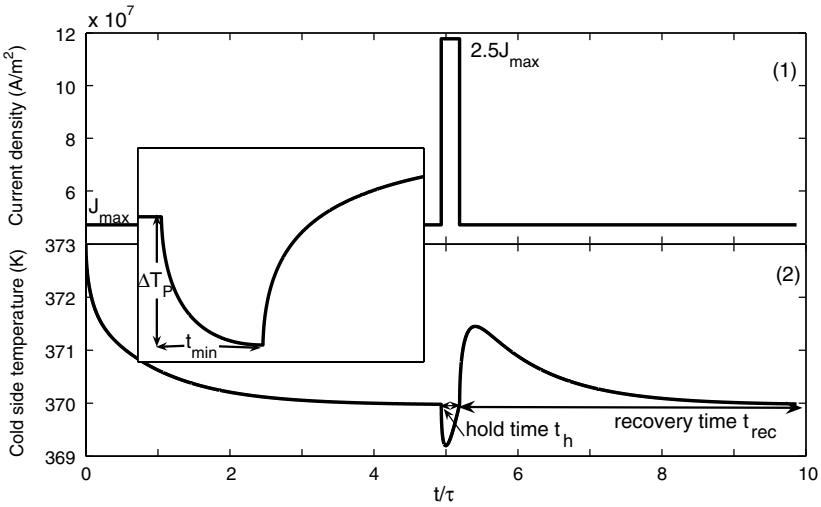

Figure 1. Subplot (1) The applied current density as a function of time; (2) the cold side temperature of homogeneous silicon as a function of time. The inset shows the cold side temperature for the case that the current returns to J_{max} right after the cold side temperature reaches its minimum.

uniform materials, (2) pulsed cooling of uniform materials and (3) steady-state cooling of graded materials. First, we apply a finite element method with very efficient tridiagonal matrix solver to obtain the solution of the steady-state equation. This allows us to explore a large number (more than 1 million) of random samples to find the optimal graded material profile. Second, a finite-difference time-domain method is used to solve the time dependent heat equation in its most general form, i.e. position- and temperature-dependent $K(x)$, $\sigma(x)$ and $S(x)$, and the pulsed cooling of graded materials is analysed.

2. Numerical methods

When electrical current flows through a single element thermoelectric cooler, temperature distribution can be calculated by a one-dimensional partial differential equation (PDE) derived from the law of energy conservation [7]:

$$\frac{\partial}{\partial x}\left(K(x)\frac{\partial T}{\partial x}\right)+\frac{J^2}{\sigma(x)}-JT\frac{\mathrm{d}S(x)}{\mathrm{d}x}=c\rho\frac{\partial T}{\partial t}. \qquad (1)$$

Here $c\rho$ is the volumetric heat capacity; σ and K are the electrical and thermal conductivities, respectively. The thermal diffusivity is $a = K/c\rho$. The three terms in the left side of equation (1) show the heat conduction, Joule heating and Peltier effects (Thomson effect as well if the Seebeck coefficient depends on temperature), respectively. Assuming there is no heat load at the cold side ($x = 0$) finite thermal resistance of the heat sink could limit the cooling performance of a thermoelectric module. In this paper we intend to focus on the cooling capacity of the thermoelectric element itself and assume that the other side ($x = L$) is in contact with a perfect heat sink with the same temperature as the environment (T_h) [7]. The boundary conditions can be written as:

$$T(L) = T_h;$$
$$\left.\frac{\mathrm{d}T}{\mathrm{d}x}\right|_{x=0^+} = \frac{SJT}{K}. \qquad (2)$$

The finite difference method is used to solve the transient state equation numerically in its general form. A scheme of forward difference in time and centred difference in space is chosen. Numerical stability is achieved when $\Delta t \leqslant (\Delta x)^2/2a$, where Δt is the time difference and Δx is the space difference [12]. In order to improve the numerical accuracy, we need to use a very small spatial grid. According to the above inequality, we have to decrease the time step simultaneously. This costs much more computation time, especially when the current is very large. Under such conditions, the temperature gradient and rate of change of temperature are so large that we need even more time steps and finer spatial grids to get accurate results. The trade-off between accuracy and computation cost is taken into account in our simulation. Figure 1 shows a typical transient response for a homogeneous silicon material. Subplots (1) and (2) are the current density and the cold side temperature in the time domain, respectively. The time unit is $\tau = 4L^2/\pi^2 a$. The reason we choose this time unit will be discussed later. J_{max} is the optimal current density that produces the maximum steady-state cooling ΔT_{max} across the thermoelectric element. After applying J_{max}, the system reaches nearly the steady-state after 5τ. Then we apply a pulse current with an amplitude $J_{pulse} = 2.5J_{max}$. The width of the current pulse is controlled so that the current returns to J_{max} when the cooling temperature becomes smaller than the steady-state ΔT_{max}. t_{min} is the time required to reach the minimum temperature and ΔT_P is the extra cooling temperature that is created by the pulse current. t_h is the hold time during which we hold the current pulse. The time that the system requires to reach the steady-state again is called the recovery time. The inset shows a different method to control the pulse width. In this case the pulse hold time is equal to t_{min}. This significantly reduces the heating overshoot and the recovery time, especially when the pulse current is large.

To verify the numerical simulations, we solve the transient equation for homogeneously doped silicon (low ZT material) analytically by the method of eigenfunction expansion [12]. The detailed derivation is described in the appendix. The temperature solution after superimposing J_{pulse} upon the

steady-state is

$$T(x,t) = \frac{T_h}{L^2}x^2 + \sum_{n=1}^{\infty} C_n(t)\sin\sqrt{\lambda_n}(L-x), \qquad (3)$$

where

$$C_n(t) = \left(C_n(0) - \frac{d_n}{a\lambda_n}\right)e^{-\lambda_n a t} + \frac{d_n}{a\lambda_n}, \qquad (4)$$

and λ_n is the eigenvalue of the heat equation. $C_n(0)$ and d_n are constants related to the initial condition and heat sources, respectively. The analytical expressions for $C_n(0)$ and d_n are shown in the appendix. $T(x,t)$ has a decaying component with a time constant $\tau = 1/\lambda_n a$. When $n \gg 1$, λ_n can be obtained by the asymptotic formula

$$\lambda_n \sim \frac{\left(n-\frac{1}{2}\right)^2\pi^2}{L^2}. \qquad (5)$$

So

$$\tau = \frac{L^2}{\left(n-\frac{1}{2}\right)^2\pi^2 a}. \qquad (6)$$

In our figures we use the time constant with the first approximated eigenvalue $\tau = 4L^2/\pi^2 a$ as the time unit. The advantage of normalizing the time with time constant τ is that the transient curve will not change with the device length. In all our calculations, we assume $L = 100\,\mu$m. For silicon, $a = 0.8\times10^{-4}\,\mathrm{m^2\,s^{-1}}$, $\tau = 50.7\,\mu$s. The analytical solution in the form of mode summation converges very fast. The $n > 1000$ modes have very little effect on the results (less than 0.1%).

Figure 2(*a*) compares the numerical and analytical calculations of the steady-state temperature profile. Figure 2(*b*) shows the transient temperature of the cold side when the current pulse magnitude is $2.5J_{max}$. The numerical simulations and analytical results are almost identical, which validates the use of this numerical method for other material systems.

3. Pulsed cooling of inhomogeneous silicon

Silicon is the basic material for very-large-scale integration (VLSI) devices. Integrated silicon thermoelectric coolers are a possible solution to the stringent thermal issues in electronic chips with nanometer size features [13, 14]. To explore the cooling limit of silicon material, we first find the optimal electrical conductivity profile of inhomogeneously doped Si using the random sampling method discussed in [11]. The optimized electrical resistivity profile and Seebeck profile are shown in figure 3. After optimization, we get the steady-state cooling temperature ~4.0 K, improved by 30% compared with the 3.1 K cooling of uniform silicon material. Upon superimposing a pulse current J_{pulse}, ΔT_p and t_{min} vary with the magnitude of the current pulse, as shown in figure 4. Numerical results are in perfect agreement with the analytical results when pulse current is less than $20J_{max}$. Figure 4 also shows that the transient cooling temperature will increase when the amplitude of the pulse current increases. However, there are two points to notice: one is that the increased cooling with current saturates after $10J_{max}$; the second is that the transient cooling will decrease if the pulse current is too large ($>50J_{max}$).

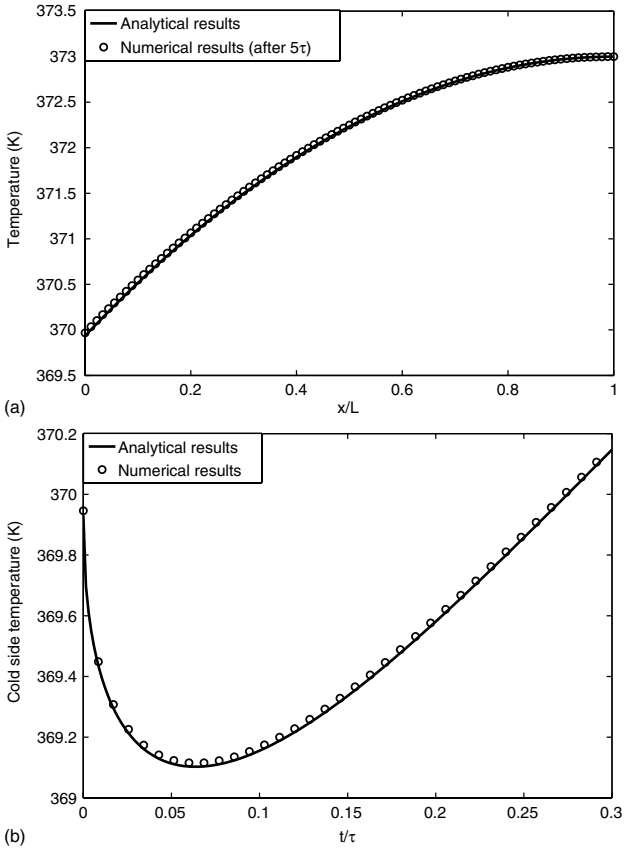

Figure 2. Comparison of the analytical and numerical results for homogeneous silicon material: (*a*) steady-state temperature distribution when optimum current is applied and (*b*) transient cooling with superimposed pulse current magnitude $2.5J_{max}$.

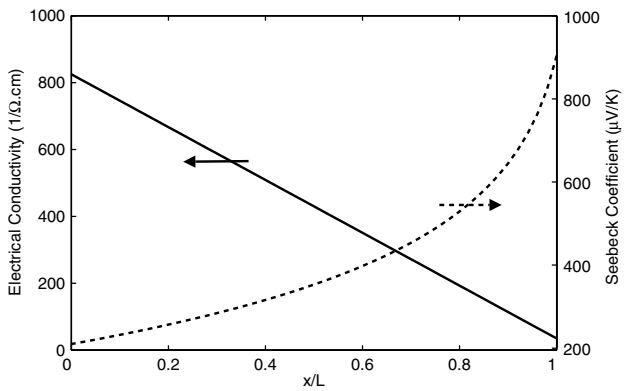

Figure 3. The optimized electrical conductivity and Seebeck coefficient profiles for graded silicon.

The extra transient cooling of inhomogeneous silicon is 1.1 K, 0.5 K less than that of homogeneous silicon when a $10J_{max}$ pulse current is injected; however, the total cooling of the inhomogeneous silicon is still 0.4 K larger than the homogeneous silicon. The cooling enhancement can be represented by the increased effective dimensionless figure-of-merit, which is given by [15]

$$ZT_h = \frac{2\Delta T}{(T_h - \Delta T)^2}T_h. \qquad (7)$$

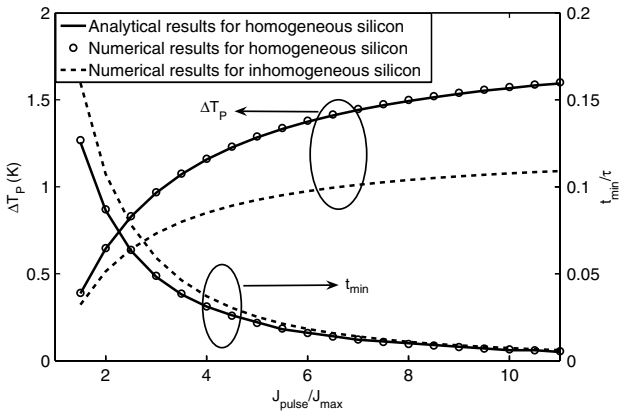

Figure 4. Comparison of the pulsed cooling of homogeneous and inhomogeneous Si. The left axis shows the maximum cooling and the right axis shows $t_{\min}$.

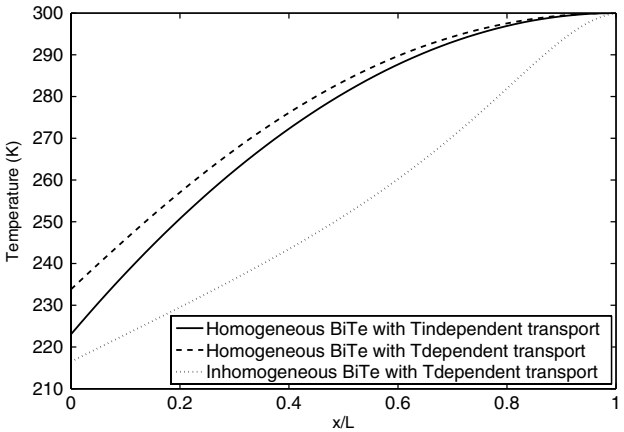

Figure 5. Steady-state temperature distribution along homogeneous and inhomogeneous BiTe leg.

For homogeneous silicon at the steady-state, $ZT_{\rm h}$ is only ∼0.017. After the electrical conductivity profile is optimized for the inhomogeneous material and pulsed cooling is used, $(ZT_{\rm h})_{\rm eff}$ is ∼0.028, with a total improvement ∼66%.

4. Pulsed cooling of inhomogeneous BiTe

BiTe is the typical thermoelectric material at room temperature. In steady-state operation, 60–70 K cooling can be achieved. Since the cooling temperature is large and material properties are changing with temperature, analytical solutions of equation (1) cannot be found even under the steady-state condition. As a first order approximation, we assume the electrical and thermal conductivities and the Seebeck coefficient do not change with temperature. The highest ZT is achieved when the mean values of the material parameters in the working temperature interval are $K = 1.83\,{\rm W\,m^{-1}\,K^{-1}}$, $S = 220\,\mu{\rm V\,K^{-1}}$ and $\sigma = 1.17 \times 10^5\,\Omega^{-1}\,{\rm m^{-1}}$. The temperature distribution can be given by an analytical solution and is plotted in figure 5 (solid line). The maximum cooling predicted in this way is 17% higher than the numerical simulation (dashed line) that takes into account the change of material properties with temperature (see [16]). Likewise, we

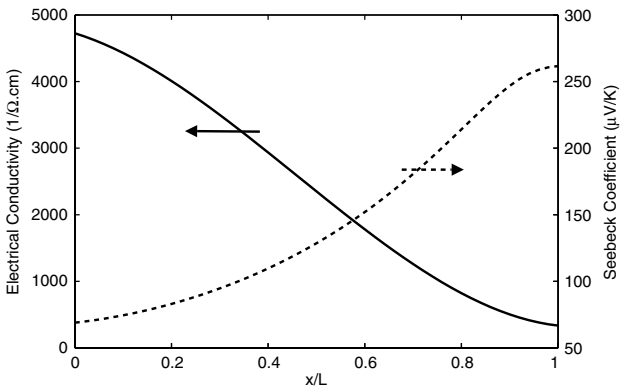

Figure 6. The optimized electrical conductivity and Seebeck coefficient profiles for graded BiTe.

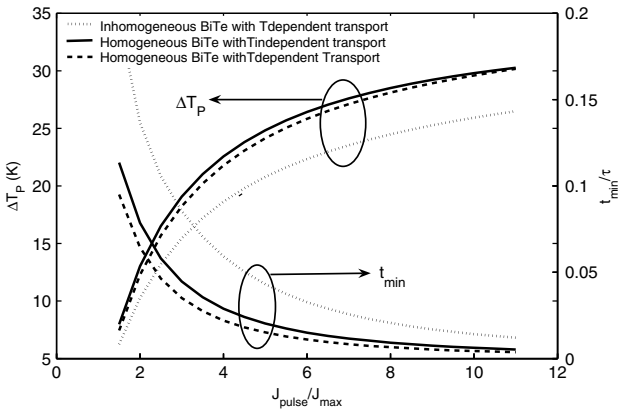

Figure 7. The transient cooling and response time as functions of pulsed current for homogeneous and inhomogeneous BiTe.

use the random sampling method to find the best electrical conductivity profile, which can be controlled by doping modulation and low temperature material growth. The best electrical conductivity and Seebeck coefficient profiles at room temperature are given in figure 6. Maximum steady-state cooling of 84 K is achieved, a 27% improvement compared with the homogeneous doping, shown by the dotted line in figure 5 [10].

Now we want to add pulsed cooling to the numerical simulation of the optimized BiTe material taking into account the temperature-dependence of material properties. The heat diffusivity of BiTe, $a = 0.7 \times 10^{-6}\,{\rm m^2\,s^{-1}}$, is smaller than that of silicon, meaning that its time constant $\tau = 4l^2/\pi^2 a = 5.8$ ms is relatively large. So we expect that BiTe would need more time to respond to the current waveform for the same material length.

Figure 7 demonstrates the extra pulsed cooling and the time to reach the minimum temperature for the three cases. It is shown that although the temperature dependence of material properties gives little correction to the extra cooling temperature, it does have a profound effect on the maximum steady-state cooling temperatures and the optimal currents as elucidated in table 1. The effective figure-of-merit of practical homogeneous BiTe under the steady-state condition is $ZT_{\rm h} \sim 0.72$. The pulsed operation of the optimized inhomogeneous BiTe gives a total cooling of ∼110 K when the pulsed current

Table 1. BiTe cooling data.

	Case I[a]	Case II[b]	Case III[c]
Steady-state cooling (K)	77	66	84
$J_{\max}L$ (A m^{-1})[d]	5.8×10^3	4.5×10^3	7.3×10^3
$J_{\text{pulse}}/J_{\max}$	10	10	10
$t_{\min}/\tau$	0.004	0.006	0.014
Additional pulse cooling (K)	30	30	26
$(ZT_{\text{h}})_{\text{eff}}$	1.66	1.38	1.82

[a] Homogeneous BiTe with T-independent transport.
[b] Homogeneous BiTe with T-dependent transport.
[c] Inhomogeneous BiTe with T-dependent transport.
[d] The value of $J_{\max}L$ is independent of the device length L.

is $J_{\text{pulse}} = 10J_{\max}$, which equivalently represents an enhanced effective figure-of-merit $(ZT_{\text{h}})_{\text{eff}} \sim 1.82$. It can also be seen that a higher pulse gives a faster response and a deeper transient cooling, which is compromised with a higher heating overshoot and a longer recovery time.

5. Conclusion

The pulsed cooling of optimized inhomogeneous thermoelectric materials can increase the cooling temperature significantly. For the practical BiTe material with $ZT_{\text{h}} \sim 0.72$, the effective figure-of-merit ZT_{h} can reach 1.82 and the total cooling temperature can be ∼110 K when a pulsed current is applied to the optimal inhomogeneous material.

Acknowledgment

This work was supported by the ONR MURI on Thermionic Energy Conversion.

Appendix A. Solving transient heat equation with third kind of boundary conditions

For low ZT materials, the cooling temperature is small and the temperature dependence of material properties is negligible. The transient thermoelectric effects can be approximated by one-dimension heat equation:

$$a\frac{\partial^2 T}{\partial x^2} + \frac{J^2 a}{K\sigma} = \frac{\partial T}{\partial t}. \tag{A1}$$

The parameters are defined as in the main text, and are assumed to be constant.

For the convenience of calculation, we flip the boundary conditions as below:

$$T(0,t) = T_{\text{h}}, \qquad \left.\frac{\partial T}{\partial x}\right|_{x=L^-} = -\frac{SJT(L,t)}{K}. \tag{A2}$$

And the initial condition is

$$T(x,0) = f(x). \tag{A3}$$

One can construct a function $r(x)$:

$$r(x) = T_{\text{h}}\left(1 - \frac{x}{L}\right)^2. \tag{A4}$$

And

$$T(x,t) = v(x,t) + r(x). \tag{A5}$$

Substituting (A5) in equations (A1)–(A3), we get the PDE for $v(x,t)$:

$$a\frac{\partial^2 v}{\partial x^2} + Q = \frac{\partial v}{\partial t}, \tag{A6}$$

with boundary conditions

$$v(0,t) = 0, \qquad \left.\frac{\partial v}{\partial x}\right|_{x=L} = -hv(L,t). \tag{A7}$$

The initial condition is

$$v(x,0) = f(x) - r(x) = g(x), \tag{A8}$$

where

$$h = \frac{SJ}{K}, \tag{A9}$$

$$\frac{2aT_{\text{h}}}{L^2} + \frac{J^2 a}{K\sigma} = Q. \tag{A10}$$

Equation (A6) can be solved by the eigenfunction expansion method. This method is discussed in [12]. The eigenfunctions are obtained from the corresponding homogeneous PDE of (A6):

$$a\frac{\partial^2 v}{\partial x^2} = \frac{\partial v}{\partial t}. \tag{A11}$$

Equation (A11) can be solved by separation of variables:

$$v(x,t) = G(t)\varphi(x). \tag{A12}$$

Substituting (A12) into (A11), we get

$$\frac{1}{aG}\frac{\mathrm{d}G}{\mathrm{d}t} = \frac{1}{\varphi}\frac{\mathrm{d}^2\varphi}{\mathrm{d}x^2} = -\lambda. \tag{A13}$$

The spatial equation is

$$\frac{\mathrm{d}^2\varphi}{\mathrm{d}x^2} + \lambda\varphi = 0, \tag{A14}$$

and the boundary conditions are

$$\varphi(0) = 0, \qquad \frac{\mathrm{d}\varphi(L)}{\mathrm{d}x} = -h\varphi(L). \tag{A15}$$

This is a regular Sturn–Liouville differential equation. Here λ must be a positive value so that the function will decay with time. Solving the equation, we get

$$\varphi(x) = c_1\cos\sqrt{\lambda}x + c_2\sin\sqrt{\lambda}x. \tag{A16}$$

Considering the boundary conditions, we get

$$c_1 = 0,$$
$$c_2\sqrt{\lambda}\cos\sqrt{\lambda}L = -hc_2\sin\sqrt{\lambda}L. \tag{A17}$$

So

$$\tan\sqrt{\lambda}L = -\frac{\sqrt{\lambda}}{h}. \tag{A18}$$

This is a transcendental equation, which can be solved by Newton's method numerically. Suppose the solutions of (A18) are known, e.g. eigenvalues $\lambda_1, \lambda_2, \lambda_3 \ldots \lambda_n$. According to the method of eigenfunction expansion [12], we obtain

$$v(x,t) = \sum_{n=1}^{\infty} C_n(t)\varphi_n(x), \tag{A19}$$

where

$$\varphi_n(x) = \sin\sqrt{\lambda_n}x. \tag{A20}$$

These eigenfunctions are all orthogonal. This is a very important property which will be used frequently in the later derivations. Now we substitute (A19) in (A6) and we obtain:

$$\sum_{n=1}^{\infty}\frac{\mathrm{d}C_n}{\mathrm{d}t}\varphi_n(x) = a\sum_{n=1}^{\infty}C_n\frac{\mathrm{d}^2\varphi_n}{\mathrm{d}x^2} + Q. \tag{A21}$$

Since the eigenfunctions are orthogonal, we get

$$\frac{\mathrm{d}C_m}{\mathrm{d}t} + a\lambda_m C_m = \frac{Q\int_0^L \varphi_m\,\mathrm{d}x}{\int_0^L \varphi_m^2\,\mathrm{d}x} = d_m, \tag{A22}$$

where

$$\int_0^L \varphi_m^2\,\mathrm{d}x = \int_0^L \frac{1-\cos 2\sqrt{\lambda_m}x}{2}\mathrm{d}x = \frac{1}{2}\left(L - \frac{\sin 2\sqrt{\lambda_m}L}{2\sqrt{\lambda_m}}\right),$$

$$\int_0^L \varphi_m\,\mathrm{d}x = \frac{1}{\sqrt{\lambda_m}}(1-\cos\sqrt{\lambda_m}L). \tag{A23}$$

Multiplying $\mathrm{e}^{\lambda_m a t}$ to both sides of (A22), and integrating with respect to time from 0 to t, we get

$$C_m(t) = \left(C_m(0) - \frac{d_m}{a\lambda_m}\right)\mathrm{e}^{-\lambda_m a t} + \frac{d_m}{a\lambda_m}. \tag{A24}$$

Using the initial condition and orthogonal property of the eigenfunctions, we obtain

$$C_m(0) = \frac{\int_0^L g(x)\varphi_m(x)\,\mathrm{d}x}{\int_0^L \varphi_m^2(x)\,\mathrm{d}x}. \tag{A25}$$

Now we have the complete solution of $v(x,t)$. From (A5) we can obtain the solution of $T(x,t)$. To be consistent with the notation in the main text, we flip back the device and get the final solution:

$$T(x,t) = \frac{T_\mathrm{h}}{L^2}x^2 + \sum_{n=1}^{\infty}C_n(t)\sin\sqrt{\lambda_n}(L-x). \tag{A26}$$

References

[1] Stilbans L S and Fedorovich N A 1958 *Sov. Phys.—Tech. Phys.* **3** 460–3
[2] Parrott J E 1960 *Solid State Electron.* **1** 135–43
[3] Snyder G J, Fleurial J P, Caillat T, Yang R and Chen G 2002 *J. Appl. Phys.* **92** 1564–9
[4] Hoyos G E, Rao K R and Jerger D 1977 *Energy Convers.* **17** 45–54
[5] Landecker K and Findlay A W 1961 *Solid State Electron.* **3** 239–60
[6] Thonhauser T, Mahan G D, Zikatanov L and Roe J 2004 *Appl. Phys. Lett.* **85** 3247–9
[7] Miner A, Majumdar A and Ghoshal U 1999 *Appl. Phys. Lett.* **75** 1176–8
[8] Muller E, Walczak S and Seifert W 2006 *Phys. Status Solidi* a **203** 2128–41
[9] Bian Z and Shakouri A 2006 *Appl. Phys. Lett.* **89** 212101-01-3
[10] Bian Z, Wang H, Zhou Q and Shakouri A 2007 *Phys. Rev.* B **75** 245208
[11] Bian Z and Shakouri A. 2006 *Proc. 25th Int. Conf. on Thermoelectrics (Vienna)*
[12] Haberman R 1998 *Elementary Applied Partial Differential Equations with Fourier Series and Boundary Value Problems* (Englewood Cliffs, NJ: Prentice-Hall) pp 215, 343
[13] Zhang Y, Zeng G and Shakouri A 2004 *Appl. Phys. Lett.* **85** 2977–9
[14] Zhang Y, Christofferson J, Shakouri A, Zeng G, Bowers J E and Croke E 2006 *IEEE Trans. Compon. Package Technol.* **29** 395–401
[15] Rowe D M 1994 *CRC Handbook of Thermoelectrics* (Boca Raton, FL: CRC Press) p 21
[16] Mahan G D 1991 *J. Appl. Phys.* **70** 4551–4